Structural Engineering and Mechanics, Vol. 5, No. 3 (1997) 269-281
DOI: http://dx.doi.org/10.12989/sem.1997.5.3.269

Elastic distortional buckling of tapered composite beams

M. A. Bradford† and H. R. Ronagh‡

Department of Structural Engineering, School of Civil Engineering,
The University of New South Wales, Sydney, NSW 2052, Australia

Abstract. The overall buckling mode in a composite steel-concrete beam over an internal support is necessarily lateral-distortional, in which the bottom compressive flange displaces laterally and twists, since the top flange is restrained by the nearly rigid concrete slab. An efficient finite element method is used to study elastic lateral-distortional buckling in composite beams whose steel portion is tapered. The simplified model for a continuous beam that is presented herein is a fixed ended cantilever whose steel portion is tapered, and is subjected to moment gradient. This is intended to give an insight into distortion in a continuous beam that occurs in the negative bending region, and the differences between the cantilever representation and the continuous beam are highlighted. An eigenproblem is established, and the buckling modes and loads are determined in the elastic range of structural response. It is found from the finite element study that the buckling moment may be enhanced significantly by using a vertical stiffener in the region where the lateral movement of the bottom flange is greatest. This enhancement is quantified in the paper.

Key words: buckling; composite beams; distortion; elasticity; tapering.

1. Introduction

Members consisting of steel and concrete elements acting compositely are now commonplace in modern engineering structures (Oehlers and Bradford 1995). The advantages that accrue to composite structures result because the compressive strength of the concrete and the tensile strength of the steel are utilised to form an economically feasible system. Further economies may be gained in composite construction if a tapered steel member is used to suit the bending moment and shear force diagrams. One such application is the increasing use of tapered steel members in continuous composite bridge girders, as shown in Fig. 1.

In designing the steel beam of a composite girder, its resistance to buckling must be evaluated. Generally, there are two types of instability that should be considered. The first is the lateral-torsional instability that may occur in unpropped construction in the sagging moment region due to the wet concrete loading during the construction phase. The second type of instability is lateral-distortional buckling (Bradford 1992) which may occur in the negative or hogging regions of the girder during live loading once composite action is achieved. It is the lateral-distortional buckling in the hogging region of a composite girder adjacent to an internal support that is treated in this paper.

† Associate Professor
‡ Research Student

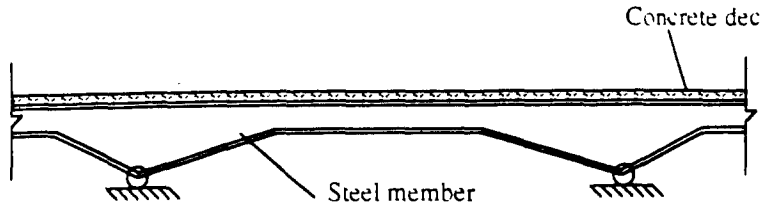

Fig. 1 Composite bridge girder.

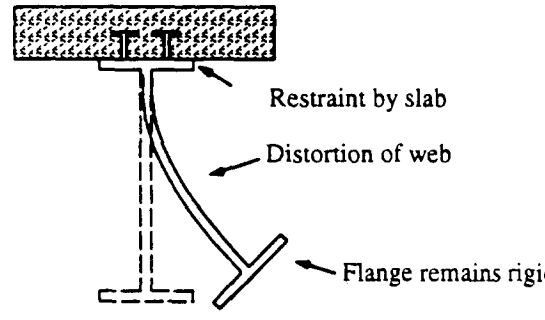

Fig. 2 Distortional buckling mode.

Lateral-torsional buckling (Trahair 1993) is a very familiar form of instability, and theoretical and numerical solutions for a wide variety of loading and support conditions are available in the literature (Trahair and Bradford 1991). This buckling may be prevented by routine application of the lateral buckling rules in modern limit states or LRFD design codes of practice. The use of these guidelines is well-known, and is not considered further here.

The second type of instability, that of lateral-distortional buckling, is far less familiar. During lateral-distortional buckling, the cross-sections of the member distort in their planes, while for lateral-torsional buckling these cross-sections buckle rigidly out-of-plane and twist in accordance with well-known Vlazov theory. In composite girders subjected to hogging bending, the bottom flange of the steel is subjected to high compressive forces as the neutral axis is above the steel mid-height, while the top flange is restrained by the concrete slab. Because of this, the only possible mode of buckling is distortional, with the bottom flange displacing laterally and twisting while the web distorts. A typical buckled cross-section is depicted in Fig. 2.

Because lateral-distortional buckling is essentially an interaction mode between local and lateral-torsional buckling, there are many factors influencing the phenomenon, and the derivation of a general solution is not straightforward. Although a closed form solution for the case of a simply supported prismatic *I*-beam was derived by Hancock, Bradford and Trahair (1980), a general and accurate solution for lateral-distortional buckling that considers the influence of such effects as tapering, moment gradient and restraint requires a numerical approach.

A recent state of the art paper (Bradford 1992) demonstrated that a considerable number of studies have been undertaken on the lateral-distortional buckling of prismatic *I*-section members using a finite element approach. Bradford and Gao (1992) and Williams, Jemah and Lam (1993) used a distortional buckling model to study the buckling of continuous composite girders which consist of a slab attached to a prismatic steel member. However, there appear to be only three studies in the open literature (Boswell 1993, Boswell and Li 1992, Lawson and Rackham 1989)

of the lateral-distortional buckling of composite beams when the steel member is tapered, as in Fig. 1. In fact, lateral-distortional buckling of tapered steel beams alone has received very little attention, with the contributions by Akay, Johnson and Will (1977) and the present authors (Ronagh and Bradford 1993, 1996) appearing to be the only available studies.

The present paper concerns the distortional buckling of tapered composite beams subjected to hogging bending, and is based on a finite element approach developed by the authors in a separate study (Ronagh and Bradford 1996). The method is quite general in that it can consider both tapering of the flanges and the web, and incorporates the effects of elastic restraints and loading remote from the shear centre. The finite element method is used herein to investigate the elastic buckling of tapered composite cantilevers under moment gradient. Although obviously not an accurate model for the buckling of continuous beams, the model is a first step to the full stability analysis of an entire continuous composite girder incorporating tapered steel members, and provides an insight into this type of instability problem.

2. Finite element buckling analysis

The finite element method developed by the authors for the distortional buckling of tapered indeterminate *I*-beams is fully outlined in Ronagh and Bradford (1996), and so details of the derivation of the stiffness matrices are not presented here for brevity. In order to perform an out-of-plane lateral-distortional buckling analysis, the in-plane stresses are required firstly, and so uncoupled in-plane and out-of-plane elements need to be developed. As the steel member is an *I*-section composed of flanges and a web, both flange and web elements have to be developed for either analysis. The member is analysed first in-plane, and the stresses determined from this analysis are input into the out-of-plane distortional model. The geometric nonlinearity is accounted for in the out-of-plane analysis by considering the loss of potential energy in the in-plane stresses as they move conservatively through the path of the out-of-plane buckling mode. This approach gives rise to the common linear eigenvalue representation (Trahair 1993) as

$$([K^{out}]-\lambda[G^{out}]) \bullet \{Q^{out}\}=\{0\} \tag{1}$$

where $[K^{out}]$ is the elastic out-of-plane stiffness matrix, $[G^{out}]$ is the out-of-plane geometric or stability matrix, $\{Q^{out}\}$ is the vector of out-of-plane displacements representing the buckling mode or eigenvector and λ is the buckling eigenvalue or load factor.

The linear eigenproblem represented in Eq. (1) is solved in two steps. Firstly, the eigenvalue is calculated by the Sturm Sequence Property (Wilkinson 1965), and then a random disturbance is applied to the loaded system for the calculation of the eigenvectors by using the method of Hopper and Williams (1977).

The elements deployed in the in-plane and out-of-plane analyses are shown in Fig. 3. Complete details of these, together with the relevant stiffness matrices, can be found in the study by Ronagh and Bradford (1996). The latter publication also shows that the method provides accurate results with only a few elements, as the convergence is rapid.

3. Modelling of the steel member

The cross-section of a composite member subjected to hogging bending is shown in Fig.

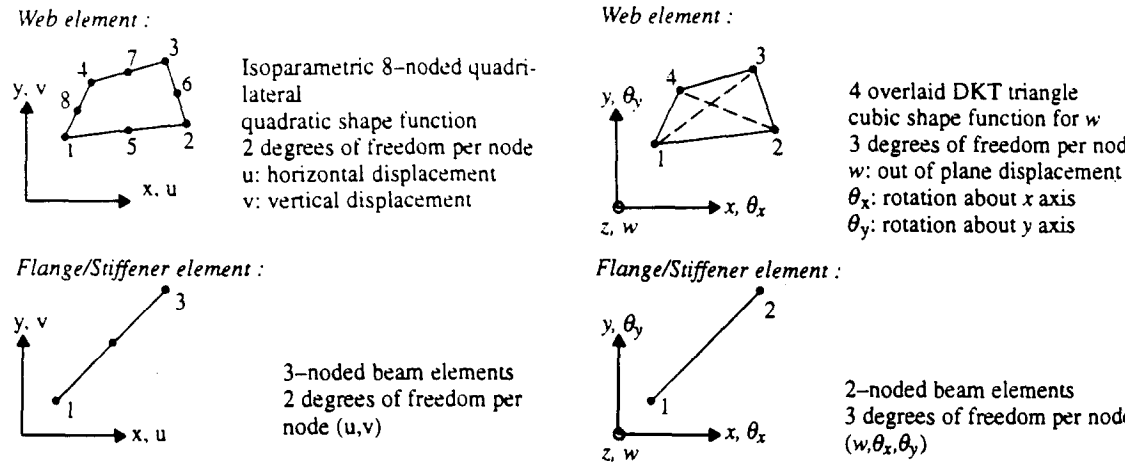

(a) In-plate elements (b) Out-of-plane elements

Fig. 3 Elements and degrees of freedom.

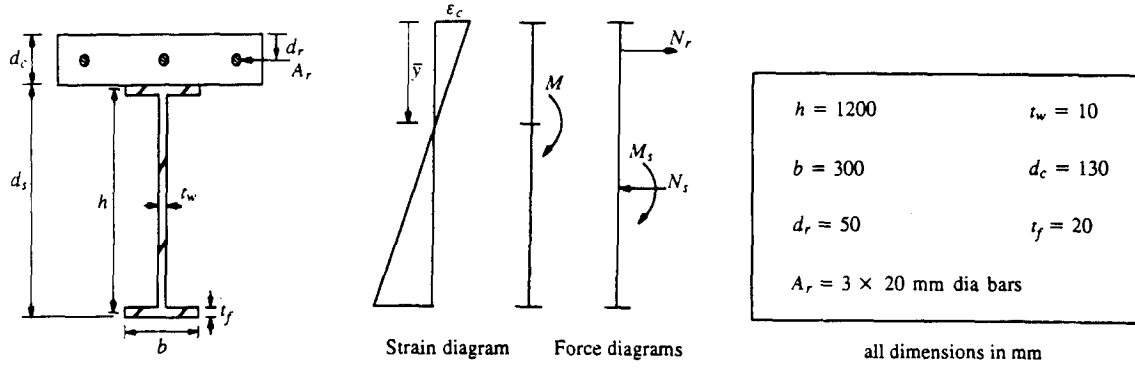

Fig. 4 Section, strain and force diagrams.

4. Assuming that the reinforcement is located at the mid-depth of the concrete slab, it can be established easily that in the elastic range the neutral axis will lie below the soffit of the concrete slab when

$$\frac{A_r}{A_s} < \frac{d_s}{d_r} \tag{2}$$

where A_r and A_s are the areas on the reinforcement and steel section respectively, and d_c and d_s are the depths of the concrete and steel sections respectively. This condition is usually satisfied in practice, as A_r is usually around 4 or 5 percent of A_s, while d_s is significantly greater than d_c. Because of this, for reasonable practical dimensions the concrete cracks throughout in the negative moment region, even if the tensile strength of the concrete is taken into account, and therefore the concrete has no effect on the cross-sectional properties.

The finite element model which is used in this study is able to model properly the steel member as an assembly of tapered web elements and flange beams. It can also model the

restraint provided by the concrete slab. This restraint is assumed to be fully rigid, so all degrees of freedom in the buckling model corresponding to the out-of-plane instability and twist of the top flange are fixed. In order to do this, the reinforcement is not introduced as a structural component, but rather its effect is treated as an applied axial loading on the steel member. As is shown in Fig. 4, and when the cross-section is subjected to a negative moment M, a tensile force N_r is induced in the reinforcement, and equilibrium requires a compressive force N_s in the steel section that is equal and opposite to N_r. The steel portion is also subjected to a moment M_s equal to the difference between the total applied moment M and the couple produced by the forces N_r and N_s.

By considering the statics of the section, M_s and N_s may be related to the applied moment M by

$$M_s=M\left(1-\frac{A_r(\bar{y}-d_r)(d_c+d_s/2-d_r)}{I_s+A_s(d_c+d_s/2-\bar{y})^2+A_r(\bar{y}-d_r)^2}\right) \tag{3}$$

and

$$N_s=M\left(\frac{A_r(\bar{y}-d_r)}{I_s+A_s(d_c+d_s/2-\bar{y})^2+A_r(\bar{y}-d_r)^2}\right) \tag{4}$$

where $\bar{y}$ is the depth of the neutral axis from the top of the slab, d_r is the depth to the reinforcement measured from the top of the slab, and I_s is the second moment of area of the steel section about its centroidal axis.

For the in-plane analysis, values of M_s and N_s need to be calculated at different points along the length. The steel member is then analysed for out-of-plane lateral-distortional buckling under the action of these stress resultants.

In order to demonstrate a general understanding of the importance of different loading parameters, the ratios N_sh/M and M_s/M were calculated for the typical cross-sectional dimensions given in Fig. 4, but using Eqs. (3) and (4) with a range of values of h. These ratios are plotted in Figs. 5(a) and 5(b). It can be seen that as h varies from 700 mm to 1200 mm, the ratio M_s/M only varies from 0.91 to 0.93, which represents a relative variation of only 2.2%. This suggests that the ratio M_s/M could be considered constant throughout a practical range of depths h without the introduction of significant error in the bending stresses. However, the values of N_sh/M vary from 0.144 to 0.121, representing a relative increase of 19%, so that the axial force cannot be considered as constant unless the effect of axial force on the stresses for a particular section is small.

In the analysis of lateral-distortional buckling, the magnitude of the compressive stress on the bottom flange, which is caused by both bending moment and axial force, is most important. The relative importance of the axial force can be ascertained from the ratio

$$\frac{\sigma_{axial}}{\sigma_{bending}}=\frac{2N_sI_s}{M_shA_s} \tag{5}$$

where σ_{axial} is the stress induced by N_s and $\sigma_{bending}$ is the stress induced by M_s at any cross-section. This ratio is calculated in Fig. 5(c), which illustrates that although the axial forces N_s vary quite significantly, their effect on the stress ratio in Eq. (5) and thus on the elastic critical load is only marginal. The axial stress σ_{axial} may thus be taken as approximately 5% of the bending stress $\sigma_{bending}$.

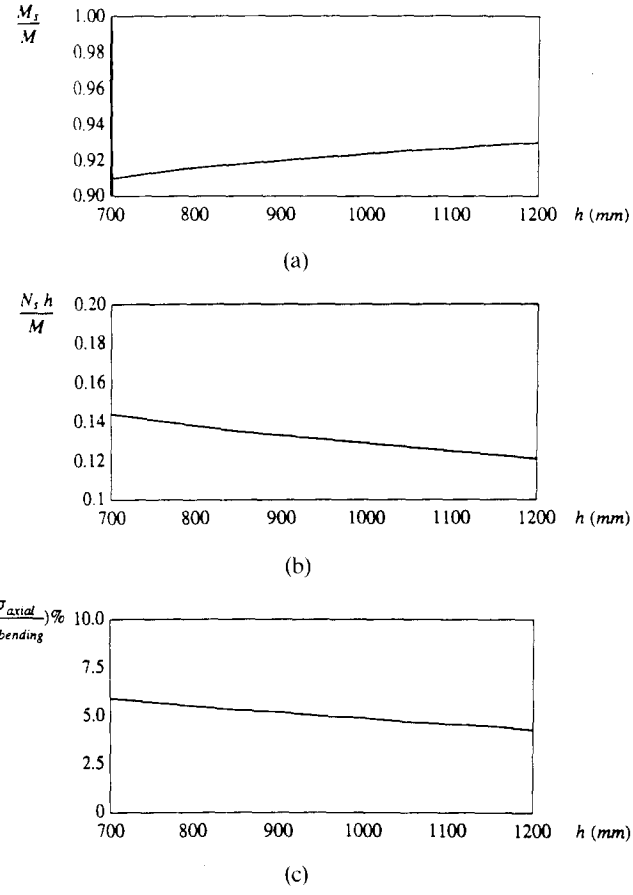

Fig. 5 Importance of different parameters on the steel section loading.

4. Studies on composite beams

4.1. Composite cantilever in uniform bending

Consider the composite cantilevers shown in Fig. 6(a). One has a prismatic steel section, while the other has a steel section with a web tapering coefficient α of 0.8, where α is the ratio of the smaller web depth to the larger web depth. The dimensions of the larger section are as shown in Fig. 4, and all of these are constant along the length of the member except the web depth which tapers linearly.

In order to analyse the lateral-distortional buckling of the cantilever, the steel member was discretised into finite elements with a mesh consisting of 12 quadrilateral elements and 24 beam elements being used for both the prismatic and tapered members, as shown in Fig. 6(c). This meshing was shown to produce results within 2% of those obtained with a very fine meshing consisting of 36 quadrilateral and 72 beam elements to which the solution converged. By using Eqs. (3) and (4), the moment acting on the steel section for the prismatic case was 0.930 M, and the axial force was 0.121 M/h. For the tapered member, however, the moment varied from 0.930 M to 0.923 M, while the axial force varied from 0.121 M/h to 0.131 M/h. These variations

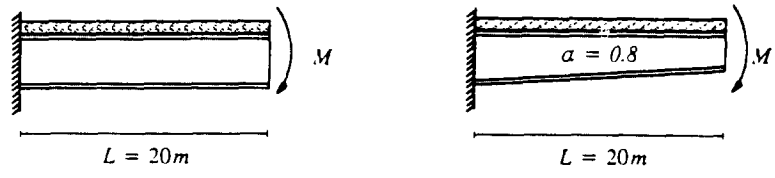

(a) Composite cantilvers

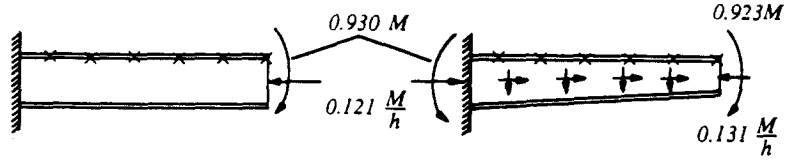

(b) Modelling of the Steel

(c) Finite element meshes

Fig. 6 Composite cantilevers under uniform moment.

were incorporated by applying the stress resultants throughout the length of the member, as shown in Fig. 6(b). This model produced an elastic critical moment of 784 kNm for the prismatic cantilever and 812 kNm for the tapered cantilever.

The discussion of the previous section has indicated that to incorporate the effects of the reinforcement, Eqs. (3) and (4) should be invoked and the stress resultants so obtained be applied to the finite element model, as was done for the previous two studies. However, as the stresses resulting from the axial forces are only marginal and the bending moment in the steel member is reasonably constant for varying values of the depth h, the following examples incorporate a constant bending moment alone in the steel member.

4.2. Tapered restrained steel beam in uniform bending

A steel cantilevered member, fixed at the top flange level and whose larger section has the dimensions of Fig. 4, has been studied. The beam was subjected to uniform bending, and values of the elastic lateral-distortional buckling moment M_{od} for this cantilever were calculated as a function of the beam length L between 10m and 40m for web tapering ratios α between 0.4 and 1.0.

The results are plotted in Fig. 7. It can be seen that in most cases the buckling moment increases as the length increases, which of course is contrary to conventional lateral-torsional buckling theory. This paradox is attributable to the buckling mode shapes of the bottom flange. The mode shapes are shown in Fig. 8 for the two extreme tapering ratios of 1.0 and 0.4, where it can be seen that for the longer beams, only the portion of the beam adjacent to the free end contributes to the buckled shape. For example, for the somewhat hypothetical case of $L=40$m,

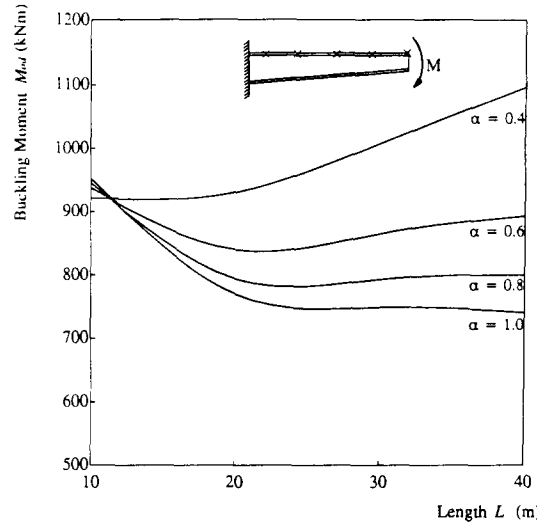

Fig. 7 Tapered steel member under uniform moment.

only the end 15m or so for $\alpha=0.4$ and 20m or so for $\alpha=1.0$ display a significant lateral movement of the bottom flange. It is also worth noting that the buckling mode shapes are not the same for the short and long beams, indicating a behaviour similar to local buckling where the local buckling half-wavelengths are more influential in the buckling load than the length of the member itself (Bradford 1990). Mode shapes corresponding to other values of α were also drawn, and these were similar to and intermediate between those of Figs. 8(a) and 8(b). Theoretically, there must be a slight kink in the curves at those particular values of the length where the mode changes its normalised shape (Bradford and Trahair 1983). For example, by considering Fig. 8 for the case of $\alpha=0.4$, it can be seen that there must be a kink somewhere between 20m and 30m from the root because the modes at these lengths have different shapes. These kinks are very small, and are not picked up in the ranges of discrete lengths chosen.

The kinks are also at locations where the mode shapes change, and their precise locations can be determined by inspecting the buckling load and eigenvector that correspond to the first or fundamental eigenvalue and second eigenvalue which can be obtained from the eigensolver. Details of this phenomenon are outlined in Bradford and Trahair (1983).

4.3. Tapered restrained steel beam under moment gradient

A steel cantilever member restrained at the top flange was considered under moment gradient in order to give an insight into the buckling behaviour of a tapered composite beam. The web depth was tapered, and the member was subjected to a moment gradient ratio β, as shown in Figs. 9 and 10, where β is the ratio of the smaller end moment to the larger end moment, and taken as positive if the member is subjected to reverse curvature.

Critical values of the elastic buckling moment M_{od} were obtained as a function of the length L for $\beta=0.5$ (Fig. 9) and $\beta=0$ (Fig. 10). It can be seen that the elastic buckling moments are much larger than for the uniform bending case shown in Fig. 5. It is interesting to note that as a consequence of the eigenmode variation discussed for uniform bending, the elastic buckling

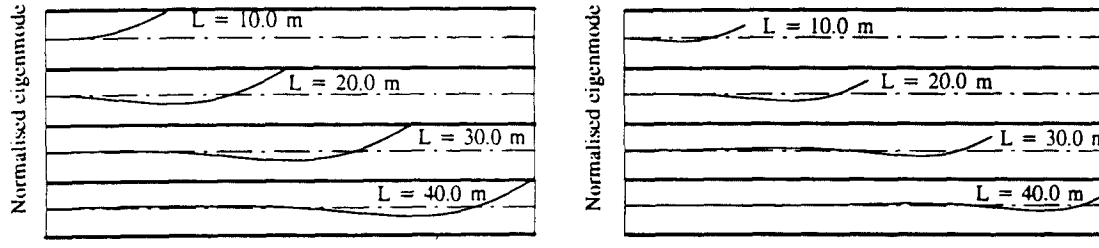

(a) Eigenmode for $\alpha=1.0$ (b) Eigenmode for $\alpha=0.4$

Fig. 8 Nomalised modes for tapered cantilever.

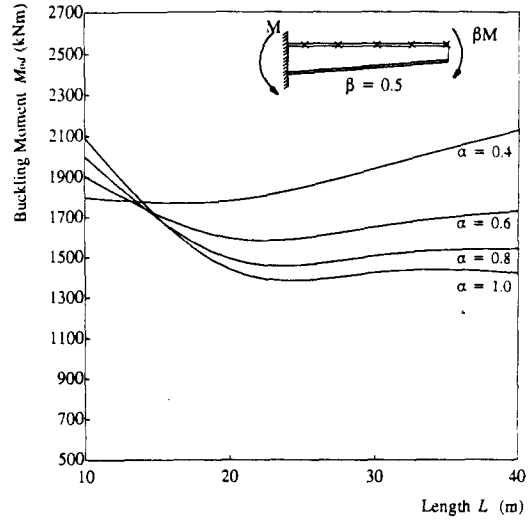

Fig. 9 Tapered steel member under moment gradient.

load actually increases in length with $\beta=0.5$ and $\alpha<1$, but this is not evident for the somewhat steeper moment gradient when $\beta=0$. Under the steep moment gradient, the region adjacent to the support is most highly stressed, and the buckling deformations were found to be greatest near the root where the resistance to the buckling deformation is greatest.

4.4. Effect of a vertical web stiffener

The effect of a vertical web stiffener on the elastic lateral-distortional buckling response of a restrained prismatic steel member was considered. It was expected that this would increase the buckling moment by restraining the bottom flange at the location of the stiffener. Vertical stiffeners may thus be advantageous in delaying lateral-distortional buckling, as well as preventing buckling of the web in shear (Trahair and Bradford 1991).

A prismatic restrained steel member with the dimensions shown in Fig. 4 was considered, but one element was used to model a 20 mm thick stiffener of the same width as the flange outstand placed on both sides of the web. The beam was subjected to uniform bending, and the coordinate x of the stiffener was varied between 0 and L.

Fig. 11 shows the values of the ratio M_{os}/M_{od} as a function of x for four different values

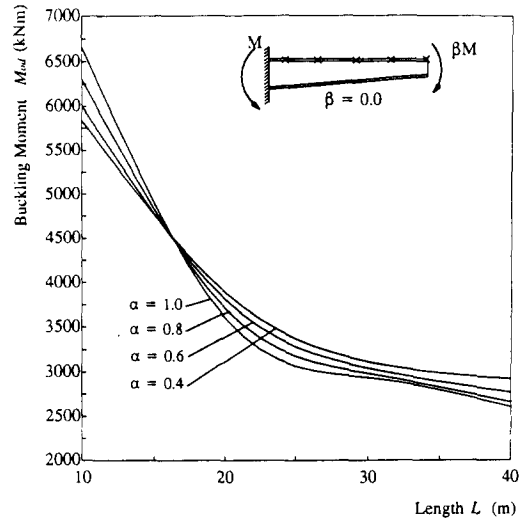

Fig. 10 Tapered steel member under moment gradient.

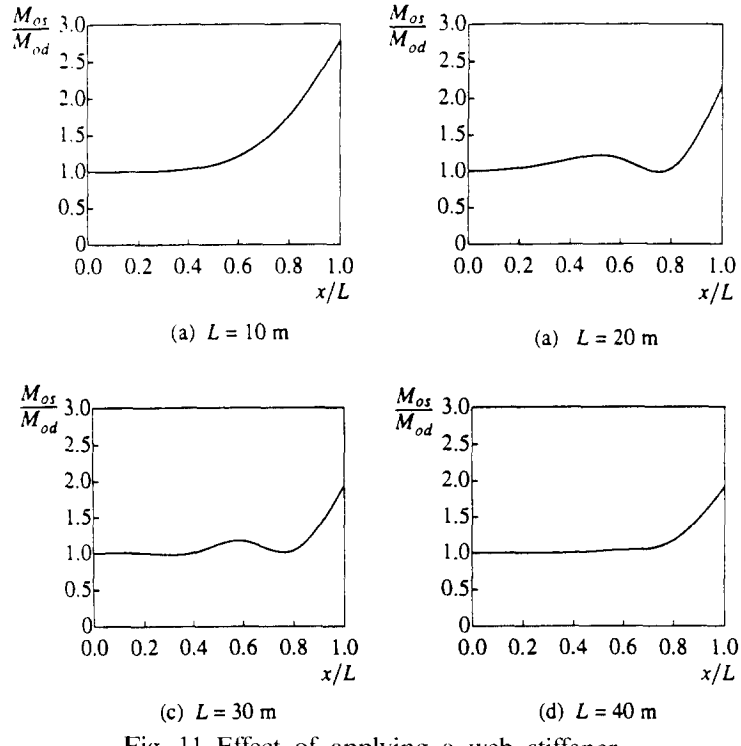

Fig. 11 Effect of applying a web stiffener.

of L, where M_{od} is the elastic lateral-distortional buckling moment without the stiffener, and M_{os} is the lateral-distortional buckling moment in the presence of the stiffener. It can be seen that the largest increase in buckling moment occurs for the shortest cantilever model, with M_{os}/M_{od} being around 2.8. There are some aberrations in the curves, showing that some stiffener locations

x are less significant, with the largest increase in buckling moment occurring when the stiffener is placed at the free end. As would be expected, a general rule is that a stiffener is most effective when placed at the point corresponding to the largest lateral movement in the eigenmode. The aberrations in Fig. 11 can thus be explained, since similar aberrations in the mode shapes occur in Fig. 8.

To clarify this, if Fig. 8(a) is compared with Fig. 11, it can be seen that placing the stiffener near the buckling nodes in Fig. 8(a) has the least effect on increasing the buckling resistance, while placing the stiffeners where the buckles in Fig. 8(a) are largest produces an enhancement in the buckling load. Similar conclusions were also found for tapered members, the solutions of which are not presented herein.

In a real composite beam, whether tapered or prismatic, the sagging moment region beyond the point of contraflexure would provide restraint to the hogging region since the bottom flange is in tension. This behaviour is akin to providing a stiffener at the free end of the cantilever, and demonstrates the benign effect of the sagging region in delaying the buckling of a composite continuous beam.

5. Design recommendation

In design, the elastic critical load must be converted to a design strength that incorporates the interaction between buckling and yielding. For hot-rolled sections, Bradford (1989) studied the inelastic lateral-distortional buckling of beams restrained by a concrete flange, and proposed a design rule that was consistent with complex finite element studies undertaken by Weston and Nethercot (1987).

In order to calculate the strength of the steel portion, the equation proposed by Bradford (1989) is

$$M_{sb}=0.8\,M_P\left\{\sqrt{\left(\frac{M_P}{M_{od}}\right)^2+3}-\frac{M_P}{M_{od}}\right\} \tag{6}$$

where M_P is the full plastic moment of the steel portion, M_{od} is the elastic lateral-distortional buckling moment of the steel portion, and the strength of the steel portion, M_{sb}, can be converted to the strength of the composite beam by use of Eq. (3). Of course, the provision of Eq. (6) is approximate, since it is based on inelastic buckling, while the section analysis in Eqs. (3) and (4) is based on elastic theory. However, it was shown by Bradford (1989) to produce reasonable results for prismatic members.

6. Concluding remarks

The elastic lateral-distortional buckling of composite cantilevers with tapered steel members has been analysed. The cantilevers were chosen as being a first step in the realistic representation of the tapered portion of a composite bridge girder continuous over an internal support. As discussed in the paper, the free end of a cantilever does not usually model the point of contra-flexure in a continuous beam, as the buckling is restrained by the tensile portion of the bottom flange in the sagging region. The cantilever model is therefore a simplification, but it does provide insight into the mechanics of the elastic instability of a tapered continuous beam. Such bridge

girders have found their way into modern construction practice, owing to modern and inexpensive fabrication techniques. The analysis was formulated to consider the steel member alone, with the concrete assumed to provide full lateral and torsional restraint to the top flange, while the effect of the tensile reinforcement was to apply a compressive force to the steel member. The steel was modelled as an assembly of tapered web elements and flange beams, and a standard eigenproblem was solved to determine the buckling loads and modes.

Elastic critical moments were calculated for a range of web taper ratios and different lengths. An interesting phenomenon observed was that the buckling moments do not always reduce with increasing length, and this was attributed to the mode shapes that develop during buckling.

The effect of deploying a vertical web stiffener was investigated, and it was found to increase the distortional buckling moment significantly. As expected, it was found that the greatest increase in buckling moment occurred when the stiffener was placed where the lateral displacements were greatest, namely at the free end of the cantilever in this case. In a continuous beam, the effect of the stiffener would be similar to the restraining effect of the sagging region beyond the point of contraflexure.

Lateral-distortional buckling of continuous composite beams is a grey area of research, and the guidelines in standard national codes of practice are either absent or questionable. The finite element method developed for this study is capable of an efficient analysis, not only of composite beams with prismatic steel members, but of composite beams with tapered steel members that are often adopted for modern bridge construction. Detailed parametric studies produced from the model, which are the subject of continuing research by the authors, should provide design guidance on this important facet of lateral-distortional instability.

Acknowledgements

This paper forms part of a programme into the behaviour of composite steel-concrete structures being undertaken at The University of New South Wales. The work presented in this study was funded by the Australian Research Council under the Large ARC Grants Scheme, whose support is gratefully acknowledged.

References

Akay, H.U., Johnson, C.P. and Will, K.M. (1977), "Lateral and local buckling of beams and frames", *Journal of the Structural Division, ASCE*, **103** (ST9), 1821-1832.

Boswell, L.F. (1993), "The distortional lateral buckling of haunched composite beams", *13th Australasian Conference on the Mechanics of Structures and Materials*, University of Wollongong, Australia, 89-95.

Boswell, L.F. and Li, Q. (1992), "Inelastic buckling of haunched composite beams", *In Structural Integrity and Assessment* (P. Stanley ed.), Elsevier Applied Science, London, 413-423.

Bradford, M.A. (1989), "Buckling strength of partially restrained I-beams", *Journal of Structural Engineering, ASCE*, **115**(5), 1272-1276.

Bradford, M.A. (1990), "Local buckling of trough girders", *Journal of Structural Engineering, ASCE*, **116**(6), 1594-1610.

Bradford, M.A. (1992), "Lateral distortional buckling of steel I-section members", *Journal of Constructional Steel Research*, **23**, 97-116.

Bradford, M.A. and Gao, Z. (1992), "Distortional buckling solutions for continuous composite beams", *Journal of Structural Engineering, ASCE*, **118**(1), 73-89.

Bradford, M.A. and Trahair, N.S. (1983), "Lateral stability of beams on seats", *Journal of Structural Engineering, ASCE.*

Hancock, G.J., Bradford, M.A. and Trahair, N.S. (1980), "Web distortion and flexural-torsional buckling", *Journal of the Structural Division, ASCE,* **106**(ST7), 1557-1571.

Hopper, C.T. and Williams, F.W. (1977), "Mode finding in nonlinear structural eigenvalue calculations", *Journal of Structural Mechanics,* **5**(3), 255-278.

Lawson, R.M. and Rackham, J.W. (1989), *Design of Haunced Composite Beams in Buildings.* The Steel Construction Institute, Ascot, U.K., Publication No. 060.

Oehlers, D.J. and Bradford, M.A. (1995), *Composite Steel-Concrete Structural Members: Fundamental Behaviour.* Pergamon Press, Oxford.

Ronagh, H.R. and Bradford, M.A. (1994), "Elastic distortional buckling of tapered I-beams," *Engineering Structures,* **16**(2), 97-110.

Ronagh, H.R. and Bradford, M.A. (1996), "A rational model for the distortional buckling of tapered members", *Computer Methods in Applied Mechanics and Engineering,* **130**, 263-277.

Trahair, N.S. (1993), *Flexural-Torsional Buckling of Structures.* Chapman and Hall, London.

Trahair, N.S. and Bradford, M.A. (1991), *The Behaviour and Design of Steel Structures.* Revised 2nd edn, Chapman and Hall, London.

Weston, G. and Nethercot, D.A. (1987), "Continuous composite bridge beams-stability of the steel compressive flange under hogging bending", *Proceedings, Stability of Plates and Shell Structures,* ECCS, Vandepitte, 47-52.

Wilkinson, J.H. (1965), *The Algebraic Eigenvalue Problem.* Clarendon Press, Oxford.

Williams, F.W., Jemah, A.K. and Lam, D.H. (1993), "Distortional buckling curves for continuous beams", *Journal of Structural Engineering, ASCE,* **119**(7), 2143-2149.

Notation

A_r	area of reinforcement;
A_s	area of steel section;
d_c	depth of slab;
d_s	depth of steel section;
$[G^{out}]$	out-of-plane geometric matrix;
h	distance between flange centroids;
I_s	second moment of area of steel section;
$[K^{out}]$	elastic out-of-plane stiffness matrix;
L	length of member;
M	applied bending moment on composite section;
M_{od}	elastic lateral-distortional buckling moment;
M_{os}	elastic lateral-distortional buckling moment in the presence of a stiffener;
M_s	moment in steel section;
N_s	axial compression in steel section;
$\{Q^{out}\}$	vector of out-of-plane buckling deformations;
x	lengthwise coordinate of stiffener;
$\bar{y}$	depth of neutral axis;
α	ratio of smaller to larger web depths;
β	ratio of smaller to larger bending moments;
σ_{axial}	stress in bottom flange due to axial force;
$\sigma_{bending}$	stress in bottom flange due to bending moment.